Endocytic pathways regulate Toll-like receptor 4 signaling and mediate crosstalk between innate and adaptive immunity.

Harald Husebye[1, 5], Øyvind Halaas[1, 5], Harald Stenmark[1,3], Gro Tunheim[2], Øystein Sandanger[1], Bjarne Bogen[2], Andreas Brech[3], Eicke Latz[4], Terje Espevik[1, 6]

[1]Institute of Cancer Research and Molecular Medicine, The Norwegian University of Science and Technology, Trondheim, Norway.

[2]Institute of Immunology, Rikshospitalet University Hospital, Oslo, Norway.

[3]Department of Biochemistry, The Norwegian Radiumhospital,Oslo,Norway

[4]Division of Infectious Diseases and Immunology, University of Massachusetts Medical School, Worcester, USA.

[5]These authors contributed equally to this work.

[6]Corresponding author: Dr. Terje Espevik, Institute of Cancer Research and Molecular Medicine, Norwegian University of Science and Technology, N-7489, Trondheim, Norway. Phone: +47 73598668, fax: +47 73598801, e-mail: terje.espevik@ntnu.no

Character count with spaces: 54929

Subject category: Immunology, membranes & transport

Key words: Toll-like receptor (TLR), endocytosis, sorting, antigen presentation

Abstract

Immune responses are initiated when molecules of microbial origin are sensed by the Toll-like receptors (TLR). We now report the identification of essential molecular components for the trafficking of the lipopolysaccharide (LPS) receptor complex. LPS was endocytosed by a receptor-mediated mechanism dependent on dynamin and clathrin and co-localized with TLR4 on early/sorting endosomes. TLR4 was ubiquitinated and associated with the ubiquitin-binding endosomal sorting protein hepatocyte growth factor-regulated tyrosine kinase substrate, Hrs. Inhibition of endocytosis and endosomal sorting increased LPS signaling. Finally, the LPS receptor complex was sorted to late endosomes/lysosomes for degradation and loading of associated antigens onto HLA class II molecules for presentation to $CD4^+$ T-cells. Our results show that endosomal trafficking of the LPS receptor complex is essential for signal termination and LPS-associated antigen presentation, thus controlling both innate and adaptive immunity through TLR4.

Introduction

The TLRs are key initiators of innate and adaptive immune responses through production of proinflammatory cytokines and chemokines, upregulation of co-stimulatory molecules and activation of antigen presentation (Akira and Takeda, 2004). The signaling receptor for LPS is TLR4/MD-2 receiving LPS from CD14. MD-2 is a small, secreted glycoprotein that associates with TLR4 in a gp96-dependent manner in the ER. MD-2 is necessary both for translocation of TLR4 from *Golgi* to the surface (Nagai *et al.*, 2002) and LPS-induced activation (Shimazu *et al.*, 1999). LPS delivered by CD14 to TLR4/MD-2 initiates a signaling cascade through the Toll/interleukin-1 receptor (TIR)-adaptors MyD88, TIRAP (also known as Mal), TRIF and TRAM which eventually leads to nuclear translocation of the proinflammatory transcription factor NFκB (Akira *et al.*, 2004). After LPS has engaged CD14, LPS is transported into *Golgi*-like structures together with TLR4 (Thieblemont and Wright, 1999;Latz *et al.*, 2002).

Excessive host responses towards LPS may lead to life-threatening complications such as septic shock, multi-organ failure and death (Waage *et al.*, 1989). Thus, it is instrumental that LPS-induced responses are finely tuned. Part of the desensitization to LPS in human monocytes is caused by downregulation of surface TLR4/MD-2 (Kitchens *et al.*, 1998). Furthermore, several negative regulators of TLR4-signaling have been reported, such as IRAK-M, short MyD88, SOCS-1, SIGIRR, ST-2, Tollip, A20, Triad3A (Liew *et al.*, 2005), and recently DAP12 (Hamerman *et al.*, 2005). Some of these negative regulators interfere with signaling molecules, whereas others, like Triad3A (Chuang and Ulevitch, 2004) and A20 (Boone *et al.*, 2004), promote ubiquitin-dependent degradation of TLRs or signaling components, respectively. Little is known about the mechanisms of the endosomal

degradation pathway of the TLRs, and if this pathway serves important functions for TLR4 and associated LPS co-receptors.

We undertook this study to delineate the mechanism by which the activated receptor complex is trafficked after engaging LPS. We have characterized the molecular mechanisms of endocytic trafficking of the LPS receptor complex and found important functional consequences of the lysosomal degradation pathway, both for the termination of signaling and the presentation of associated antigens to the $CD4^+$ T helper cells.

Results

LPS downregulates plasma membrane TLR4 and both appear on endosomes

During the first hours of incubation with LPS a gradual decrease in plasma membrane TLR4 was observed in monocytes (Fig. 1a). This occurred concomitantly with formation of endosome-like structures containing LPS^{Cy5} (Fig. 1b, upper panel). At later time points, LPS accumulated in the perinuclear area (Fig. 1b, lower panels). For the detection of TLR4, a TLR4 antibody (anti-$TLR4^{A546}$) was added simultaneously with fluorescent LPS (LPS^{OG}) to monocytes. Co-localization of TLR4 and LPS was observed in microdomains on the endosomal limiting membrane one hour after stimulation (Fig. 1c).

We went on to study the localization and transport of TLR4 fused to YFP ($TLR4^{YFP}$) in live HEK293 cells expressing the co-receptors MD-2 and CD14 using confocal microscopy and LPS^{CY5} for stimulation. In unstimulated cells, $TLR4^{YFP}$ was found in the endoplasmic reticulum, at the plasma membrane, as a large pool in the *Golgi* area and sporadically on endosomal structures (Fig 2a). Following LPS stimulation, endosomes showing LPS and TLR4 co-localization appeared within 15 minutes, suggesting active endocytosis (Fig. 2a, b). Addition of LPS increased the number of TLR4 containing endosomes seven-fold within the first 40 minutes of stimulation and this increase was dependent on the co-receptor MD-2 (Fig 2b, c). Although we found endosomes containing TLR4 and LPS in the absence of MD-2, the presence of MD-2 enhanced the process, and also promoted aggregation of TLR4 in patches on the endosomes, as seen in Fig. 1c and upper right panel of Fig. 2a. CD14 greatly increased both binding to the surface and uptake of LPS, as has previously been reported (Kitchens *et al.*, 1998;Latz *et al.*, 2002).

LPS and TLR4 are trafficked to early/sorting endosomes

We further characterized the compartments into which LPS and TLR4 were sorted. Since LPS binding to the surface was only detected in cells expressing CD14, we subsequently used LPS binding as a marker for cells that had been successfully transfected with the CD14 plasmid. To characterize the TLR4 positive endosomes, cells were transfected with plasmids encoding CD14 and a CFP chimera containing tandem FYVE domains from the mouse Hrs ($2\times FYVE^{CFP}$). This construct binds phosphatidylinositol-3-phosphate (PI3P) that is highly enriched on early/sorting endosomes (Gaullier *et al.*, 1998;Simonsen *et al.*, 1998;Gillooly *et al.*, 2000). Within the first hour of LPS stimulation, most endosomes containing TLR4 and LPS were FYVE positive (Fig. 2d). Endosomes containing TLR4 and LPS, and identified by $2\times FYVE^{CFP}$, were also positive for transferrin (Fig. 2e, Supplementary Figure 2). Transferrin is endocytosed in a clathrin-dependent manner and sorted on early/sorting endosomes. In cells stimulated for longer periods, TLR4 and LPS appeared on endosomes being FYVE negative (data not shown). TLR4 showed extensive co-localization with LPS in all compartments. The localization of TLR4 to early endosomes was also confirmed by staining fixed cells with an antibody to the early endosomal marker EEA1 (data not shown) or by co-transfecting the cells with a truncated but functional EEA1 (Stenmark *et al.*, 1996) fused to CFP ($EEA1^{CFP}$). In unstimulated cells TLR4 was present on small $EEA1^{CFP}$ positive endosomes that grew significantly larger in size after LPS stimulation (Supplementary Figure 1a). These EEA1 positive endosomes, like the FYVE positive endosomes, contained a substantial amount of LPS and TLR4 on the limiting membrane. In addition, images were obtained demonstrating apparent fusion events between LPS positive endosomes (Supplementary Figure 1b and Supplementary Movie). Taken together, our data show

that LPS and TLR4 are trafficked to early/sorting endosomes and that LPS induced signaling increases the size of these endosomes probably by endosome-endosome fusions.

LPS is endocytosed by a receptor mediated mechanism involving dynamin and clathrin

Receptor mediated endocytosis is often classified by being clathrin-dependent (through coated pits as seen with transferrin) or clathrin-independent (through caveoli or lipid rafts as seen for many glycosylphosphatidylinositol (GPI)-anchored proteins). Both mechanisms are dependent on dynamin, whereas (macro)pinocytosis is dependent on actin (Nichols, 2003). Dynamin proteins are GTPases that are essential for budding of vesicles from the plasma membrane and from recycling endosomes. Whereas transmembrane proteins contain sorting information in the cytosolic domain, GPI-anchored proteins (like CD14) have in general been shown to either be co-endocytosed with the transmembrane proteins, or pinocytosed together with fluid phase contents (Mayor and Riezman, 2004). We next investigated whether LPS endocytosis was dependent on dynamin using constructs of dynamin II wild type (WT) and dominant negative dynamin II (Dyn K44A) (Damke *et al.*, 1994). Cells expressing $TLR4^{YFP}$/ MD-2 were co-transfected with CD14 and dynamin WT or Dyn K44A, and investigated by confocal microscopy (Fig. 3a). Fluorescent transferrin and LPS were added together for selection of cells with a dynamin knock down phenotype. LPS and transferrin uptake were not affected in the dynamin WT transfectants (Fig. 3a, left panel), whereas in the Dyn K44A transfectants (Fig. 3a, right panel) a clear accumulation of transferrin on the plasma membrane was observed and, as a consequence, reduced transferrin uptake (Damke *et al.*, 1994). In DynK44A

transfectants, total LPS uptake was reduced to about 18% of the uptake in dynamin WT transfectants (Fig. 3b), supporting that LPS is endocytosed by a receptor-mediated vesicular mechanism.

Clathrin is a scaffold protein involved in assembly of selected transmembrane proteins in invaginations called clathrin-coated pits. We knocked down clathrin heavy chain by siRNA technology (Motley *et al.*, 2003) in HEK293 cells expressing $TLR4^{YFP}$/MD-2 including a non-interfering scrambled RNA duplex (Bache *et al.*, 2003) as control. Following siRNA treatment the cells were transfected with CD14 and the uptake and distribution of LPS and transferrin investigated (Fig. 3c). The introduction of control siRNA did not affect LPS and transferrin uptake (Fig. 3c, left panel) whereas clathrin siRNA resulted in significant accumulation of both transferrin and LPS at the plasma membrane in these cells (Fig. 3c, right panel). Cells showing accumulation of transferrin at the plasma membrane were scored as clathrin knock down transfectants. In these cells, LPS did not appear on endosomes during the first 40 minutes of stimulation (Fig. 3c, d). At later time points LPS appeared on large endosomes also positive for transferrin (data not shown), suggesting an additional but slower clathrin-independent uptake mechanism. As we found siRNA against clathrin to be very effective in inhibiting both transferrin and LPS uptake, our results show clathrin to be an essential component for the early endocytosis of the LPS receptor complex.

TLR4 is ubiquitinated and associates with Hrs.

The targeting of transmembrane proteins to lysosomes is determined by tyrosine phosphorylation and di-leucin motifs of which there are candidates in TLR4. Tyrosine based motifs (YXXΦ) are found in positions 587 (YDAF), 622 (YRDF) and

707 (YLEW), whereas a di-leucine motif ([DE]XXXL[LI]) is found in position 697 (ELYRLL), both recognized by adaptor protein (AP) complexes involved in the initial phase of endocytosis (Bonifacino and Traub, 2003). A major additional mechanism for endocytosis and lysosomal targeting of transmembrane proteins is by the covalent attachment of one or more ubiquitins to lysines to the cytosolic domain (Hicke, 2001;Raiborg *et al.*, 2003). A recent report showed that the E3 ubiquitin ligase Triad3A was involved in degradation of TLRs (except TLR2) (Chuang *et al.*, 2004). Thus, we wanted to address if LPS induced ubiquitination of TLR4 and if this had any effect on endocytosis and degradation of TLR4. We found that TLR4 ubiquitination was both constitutive and enhanced by LPS in HEK293 cells expressing $TLR4^{YFP}$/MD-2 (Fig. 4a). In monocytes, a weak increase in ubiquitination of TLR4 was observed at 1 hour of LPS stimulation, followed by a reduction after 3 hours (Fig. 4b). TLR4 was ubiquitinated in cells transfected with *c*-myc tagged Ub wild type (UbRGG) but not in cells transfected with a *c*-myc tagged non-functional Ub (UbR) lacking the two C-terminal glycines required for covalent conjugation to proteins (data not shown) (Stang *et al.*, 2004). There was, however, no effect of UbR on uptake of LPS within the first hour of stimulation (data not shown) suggesting that LPS uptake is Ub-independent. Ubiquitin ligases are recruited by their SH2 domains to tyrosine phosphorylated targets, and we found that TLR4 was indeed tyrosine phosphorylated in response to LPS (data not shown). These data suggest that although TLR4 is ubiquitinated as a response of LPS stimulation, ubiquitination is not required for the initial endocytosis of the LPS receptor complex.

Hrs is located to clathrin-coated microdomains of the early/sorting endosomal limiting membrane where it is involved in the recognition and targeting of ubiquitinated protein cargo to the lysosomal degradation pathway by promoting

translocation of the target proteins to the lumen of endosomes forming multivesicular bodies (MVB) (Gruenberg and Stenmark, 2004). Hrs has recently also been shown to associate with phagosomes and aid in fusion with lysosomes (Vieira *et al.*, 2004). We investigated the involvement of Hrs in TLR4 trafficking in monocytes and in HEK293-TLR4^{YFP}/MD-2 cells transiently transfected with *c*-myc tagged Hrs. In monocytes Hrs constitutively associated with TLR4, however the association increased transiently after 1 hour of LPS stimulation (Fig. 4b). Control IgG did not co-precipitate TLR4 (Fig. 4b) or Hrs (data nor shown). The TLR4 immunoprecipitated with Hrs was slightly larger and appeared more smeared than the mature form of TLR4 (Fig. 4b, middle), possibly because Hrs interacts mainly with multiple ubiquitins on the intracellular domain of TLR4. Also in HEK293 cells overexpressing *c*-myc-Hrs we found that TLR4 co-precipitated with Hrs (Fig. 4c) in an LPS-inducible manner, whereas control IgG did not (control C1, Fig 4c). The upper band in Figure 4c represents the c-myc tagged Hrs and the lower band is the endogenous Hrs as shown by co-migration with the endogenous Hrs from non-transfected HEK293 cells (control C2, Fig 4c). Importantly, a moderate overexpression of c-myc Hrs (here estimated to be less than 3 times the endogenous level) lead to a rapid decrease in the amount of total cellular TLR4 after addition of LPS, whereas the amounts of Hrs and tubulin were unaffected (Fig. 4c). This result is in accordance with a recent paper (Scoles *et al.*, 2005), who demonstrated that overexpression of Hrs (eg. less than 10 times the endogenous level) results in a rapid decrease in the EGFR levels upon stimulation with EGF. Furthermore, TLR4^{CFP} and Hrs^{YFP} were co-localized on discrete microdomains on the endosomal limiting membrane following LPS stimulation (Fig. 4d).

TLR4 is trafficked to lysosomes for degradation

Next, we investigated the effect of chloroquine and lactacystin on TLR4 levels following LPS stimulation in HEK293 cells expressing $TLR4^{YFP}$/MD-2 and transfected with CD14. Chloroquine inhibits maturation of early endosomes to lysosomes by inhibiting acidification and thus preventing lysosomal degradation (Mellman *et al.*, 1986). Lactacystin is an irreversible proteasome inhibitor. Previous studies have shown that cellular TLR4 is present in two different sizes, the larger is a 130 kDa heavily glycosylated, MD-2-dependent, surface-translocated form and the smaller is a 110 kDa partially glycosylated form found predominantly in *Golgi* (Nagai *et al.*, 2002;Ohnishi *et al.*, 2003). LPS seemed to increase the total cellular TLR4 after 10 hours which may be due to increased transcription of the CMV-promoted TLR4-YFP constructs by LPS (Lee *et al.*, 2004). However, 1 hour of LPS stimulation did not increase the TLR4 level. Treatment with chloroquine resulted in a significant cellular accumulation of both forms of TLR4 as early as 1h after LPS (Fig. 5a). Interestingly, lactacystin reported to block Triad3A-mediated degradation of TLR9 (Chuang *et al.*, 2004), did not cause the same accumulation of $TLR4^{YFP}$ in LPS stimulated cells (Fig. 5a). LY294002 (LY) inhibits the PI3-kinase enzymes responsible for the formation of the cellular PI3P controlling endosome fusions (Simonsen *et al.*, 1998) and the formation of intraluminal vesicles in late endosomes/MVBs (Futter *et al.*, 2001). PI3-kinase activity is also required for the recruitment of Hrs to endosomal membranes (Komada and Soriano, 1999;Urbe *et al.*, 2000). Cells treated with LY and stimulated with LPS showed a dramatic increase in the level of $TLR4^{YFP}$ after 10 hours of LPS stimulation compared to LPS stimulated cells treated with control vehicle (Fig. 5b). Altogether these data suggest that endosomal sorting and acidification are required for degradation of TLR4.

Furthermore, we investigated the involvement of Hrs in TLR4 degradation by knocking down the endogenous level of Hrs by siRNA technology (Bache *et al.*, 2003). Hrs siRNA-treated HEK293 cells expressing $TLR4^{YFP}$/MD-2 and transfected with CD14 showed an increased levels of both the large fully glycosylated and the partially glycosylated $TLR4^{YFP}$ form compared to the cells treated with control siRNA (Fig. 5c, upper panel). Our results suggest that ubiquitinated TLR4 associates with Hrs directing the activated TLR4 to lysososomes for degradation. This result is in contrast to TLR9 that has been reported to be degraded by proteasomes after ubiquitination by the Triad3A ubiquitin ligase (Chuang *et al.*, 2004).

Inhibition of the endosomal pathway increases LPS induced NFκB activation

After describing mechanisms of the TLR4 sorting through the endosomal pathway, we investigated the role of this pathway on LPS induced NFκB activation. By comparing the effect of wild type *versus* dominant negative constructs for the trafficking components dynamin II (dynamin WT *vs.* Dyn K44A) and ubiquitin (UbRGG *vs.* UbR) we found that the reduced endocytic activity caused by Dyn K44A, or saturation of Ub-interacting proteins with the non-functional UbR, caused increased NFκB activation compared to overexpression of the WT constructs (Fig. 5d and Supplementry Figure 3). This result strongly supports that signaling is initiated at the plasma membrane (Latz *et al.*, 2002;Ahmad-Nejad *et al.*, 2002) and that endocytosis and lysosomal targeting of TLR4 limit NFκB activation. Additional arguments for this conclusion was also obtained in knock down experiments of Hrs with siRNA showing a 70% increase in LPS induced NFκB activation compared to control (Fig. 5e and Supplementry Figure 3). Furthermore, by knocking down an essential component (HCRP1) of the endosomal sorting complexes required for

transport-I (ESCRT-I) with siRNA (Bache *et al.*, 2004), the LPS (10 ng/ml) induced NFκB activation increased by 245 % compared to the siRNA control (Fig. 5e). These data suggest that dynamin, ubiquitin, Hrs and HCRP1 (i.e. ESCRT-I) are involved in desensitizing the cell after LPS activation, most likely through endocytosis and lysosomal degradation of the activated LPS receptor complex.

Antigens associated with the LPS receptor complex are presented on HLA class II to CD4$^+$ T helper cells

Time-lapse series of LPS stimulated monocytes showed that LPS overlapped with dextran in dynamic tubular structures protruding from the perinuclear area after 3-5 hours of incubation (data not shown). These protrusions were directed towards the plasma membrane as has been described for MHC class II containing lysosome-like tubulae after LPS stimulation in dendritic cells (Boes *et al.*, 2002), a phenotype not observed in HEK293 cells. By counterstaining HEK293 cells expressing TLR4^{YFP}/MD-2 transfected with CD14 with an antibody against the late endosomal/lysosomal marker protein LAMP-1, we observed that TLR4^{YFP} was present in the lumen of late endosomes/MVB`s following LPS stimulation (Fig. 6a). Treatment of stimulated live cells with LysoTracker Red showed that TLR4^{YFP} and LPS^{CY5} co-localized at the limiting membrane and in the lumen of non-acidic endosomes (Fig. 6b). Intraluminal TLR4^{YFP} was lost following endosomal acidification whereas LPS^{CY5} was still detectable. Since TLR4 and LPS/CD14 are directed through the endocytic compartments to lysosomes for degradation, associated antigens may be presented on HLA class II to CD4$^+$ T cells. We performed antigen presentation assays using mouse antibodies to TLR4 (HTA125), CD14 (5C5) and MD-2 (IIC2) and proliferation of a CD4$^+$ T cell specific for the mouse κ-light chain-

derived peptide Cκ$^{40-48}$ presented on HLA-DR4 (Schjetne *et al.*, 2002) in an LPS free system. This system is designed for functional testing of the class II presentation pathway by providing a read-out for lysosomal antigen processing, loading and presentation in primary human cells. We found efficient presentation of the antibody-derived peptide (Fig. 6c) suggesting that TLR4, MD-2 and CD14 were directed to a functional class II loading compartment, most commonly ascribed to MVB (Peters *et al.*, 1991). This result implies that the LPS receptor complex, TLR4/MD-2/CD14, not only signals the presence of microbes but also assists in directing the endocytosis of antigens for presentation on class II molecules to T helper cells.

Discussion

Molecular mechanisms involved in sorting of the LPS receptor complex

The TLR4 agonist, LPS, is a potent immune stimulator that can cause sepsis. TLR4 signaling is under tight regulatory control at multiple levels and several inhibitors of TLR4 signaling have now been described. Internalization of receptors regulates signal transduction (Di Guglielmo *et al.*, 2003), however, little attention has been devoted to mechanisms and functional consequences of the endocytic uptake of the LPS receptor complex. In this study we have characterized the uptake of LPS and the sorting of the LPS receptor complex from the plasma membrane to the late endosomes/lysosomes and explored functional consequences of this endosomal pathway.

Internalization of membrane receptors occurs both through clathrin- and caveolae/raft-mediated pathways. The EGF receptor is internalized within minutes after ligand addition by a clathrin mediated pathway (Le and Wrana, 2005) whereas the IL-2 receptor appears to be taken up by a lipid raft dependent manner (Lamaze *et al.*, 2001). Previous reports have shown that CD14 is located in lipid rafts and that a fraction of TLR4 moves into the lipid raft domain after LPS stimulation, a result suggesting a clathrin-independent uptake of the LPS receptor complex (Triantafilou *et al.*, 2004). Furthermore, Kitchens *et. al.* reported that the CD14-mediated uptake of LPS occurs by both clathrin-dependent and -independent pathways (Kitchens *et al.*, 1998). Knocking down clathrin by siRNA results in a significant inhibition of EGF uptake at low EGF doses and less effective at higher EGF doses (Sigismund *et al.*, 2005). Our results using siRNA for clathrin clearly demonstrate that the early phase (up to 40 min) of LPS internalization is predominantly clathrin-dependent, whereas clathrin-independent pathways operate at later time points.

Monoubiquitination serves an important role in sorting membrane proteins through the endosomal pathway (Raiborg *et al.*, 2003), whereas polyubiquitination is the recognition signal for proteasomal degradation (Marmor and Yarden, 2004). As mentioned above, Triad3A has been reported to be an E3 ubiquitin ligase that promotes proteasomal degradation of TLR9 (Chuang *et al.*, 2004). Triad3A-mediated ubiquitination does not seem to play a role in the lysosomal degradation pathway as the effect of this ligase on TLR9 degradation is dependent on proteasomal, but not lysosomal activity (Chuang *et al.*, 2004). We observed increased ubiquitination of TLR4 upon LPS activation both in monocytes and in genetically engineered cells. Hrs has an essential role in sorting ubiquitinated proteins into clathrin-coated microdomains of early endosomes (Raiborg *et al.*, 2002) and Hrs has interacting domains for PI3P (the FYVE domain), clathrin and ubiquitin (Bache *et al.*, 2003). We provide evidence for Hrs interaction with TLR4 on endosomes and that this interaction was increased upon LPS activation. Thus, Hrs seems to play an important role in the initial steps of TLR4 sorting to the endosomal pathway. A part of the LPS receptor complex also traffics from the plasma membrane to the *Golgi* (Latz *et al.*, 2002), and this pathway may either go directly from the plasma membrane or through the early/sorting endosomes. Whether Hrs also plays a role in TLR4 trafficking to the *Golgi* apparatus is not known. Another protein, Tollip, has been shown to inhibit LPS-induced NFκB activation (Zhang and Ghosh, 2002) by a mechanism requiring localization to endosomes or activated plasma membranes and through binding of ubiquitinated cargo and recruitment to clathrin-coated microdomains (Katoh *et al.*, 2004), not unlike Hrs. It is thus likely that redundancy exists in the machinery that ensures that inflammatory signals are shut off to avoid hyperinflammation and the accompanied adverse effects.

Endosomal trafficking of the LPS receptor complex leading to lysosomal degradation and signal termination was consistently demonstrated in the HEK293-TLR4 cells. Our results suggest that a similar pathway of LPS receptor endocytosis and degradation also operates in monocytes. Firstly, LPS induced a clear downregulation of TLR4 on the plasma membrane with subsequent localization of LPS and TLR4 to endosomes. Secondly, ubiquitination of TLR4 was constitutive, weakly increased after 1 hour of LPS stimulation and markedly decreased after 3 hours. Finally, TLR4 associated with Hrs and this association was transiently increased at 1 hour of LPS stimulation. Direct evidence for LPS induced lysosomal degradation of TLR4 in monocytes was difficult to obtain probably due to a high turnover rate for TLR4. However, antibodies towards TLR4, MD-2 and CD14 were degraded in MVB/lysosomes since an antibody derived peptide was loaded onto HLA class II (Fig. 6c). Thus, it is likely that the pathway of endosomal degradation of TLR4 that we demonstrated in the HEK293 TLR4 cells also takes place in monocytes.

Inhibition of endocytosis and endosomal sorting increase LPS induced proinflammatory signaling

Our studies provide evidence that sorting the LPS receptor complex through the endosomal pathway has important functional consequences. We observed a striking increase in LPS signaling when proteins involved in endosomal trafficking and maturation were inhibited. By reducing the amount of functional ESCRT-I, which associates with Hrs and is involved in the sorting of ubiquitinated proteins into multivesicular bodies (Bache *et al.*, 2002), a more than 2 fold increase in the LPS signaling was observed. Inhibition of ubiquitination and depletion of Hrs or ESCRT-I resulted in increased LPS signaling. Furthermore, overexpression of Hrs lead to a

significant increase in LPS induced TLR4 degradation. From these results it is apparent that LPS signaling starts at the plasma membrane, however, signaling is likely to continue along the endosomal pathway until an Hrs and ESCRT-I mediated translocation of TLR4 to the luminal side of endosomes has taken place. This view is also supported by confocal imaging showing the presence of the signaling adapters MyD88 and TRAM at the plasma membrane and on endosomes in LPS stimulated cells (H. Husebye and T. Espevik, unpublished results). Signaling on endosomes is also reported for TGF-β which is taken up by a clathrin-dependent mechanism and trafficked into early endosomes where the signaling component SARA is enriched (Di Guglielmo *et al.*, 2003).

The LPS receptor complex links innate and adaptive immunity

A very important consequence of the trafficking of the LPS receptor complex described in this paper is that antigens associated with the LPS receptor complex are directly transported to the antigen presentation machinery for presentation to $CD4^+$ T helper cells. The loading of antigens on class II molecules occurs by fusion of limiting and intraluminal membranes in MVBs (Peters *et al.*, 1991) resulting in exchange of the class II inhibitory peptide (CLIP) with lysosomal peptides derived from processed exogenous proteins. This is also highly relevant for other suggested ligands of TLR4, like heat shock proteins, viral proteins (Akira *et al.*, 2004) and co-trafficked antigens, by providing a direct link between activation of innate and acquired immune cells. This may be exploited in design of synthetic vaccines aimed at the $CD4^+$ T helper cell population, as has been shown for conjugated complexes of lipoproteins and immunogenic peptides acting through TLR2 (Jackson *et al.*, 2004).

Altogether, our results strongly support that distinct components of the endocytic pathway inhibit inflammatory signals induced by TLR4 and that long-lived information is simultaneously passed on to the adaptive branch of the immune system.

Materials and methods

Reagents

LPS (0111:B4) from *Escherichia coli* was purchased from Invivogen. Cy5- and OregonGreen (OG) labeling of LPS was performed as previously described (Latz *et al.*, 2002). Alexa-labeling of antibodies was performed according to the manufacturer's protocol (Invitrogen). Alexa^{546}-labelled transferrin and LysoTracker Red were purchased from Invitrogen. LY294002 and lactacystin were purchased form Calbiochem. Chloroquine was purchased form Sigma. Mouse antibodies used: anti-GFP (JL-8) (Clontech), anti-TLR4 (HTA125) was kindly provided by Dr. Kensuke Miyake (Saga Medical School, Japan) (Yang *et al.*, 2000), anti-*c*-Myc (9E10) (BD Bioscience), anti-ubiquitin-protein conjugates (FK2) (Affiniti Research), anti-LAMP1 (R&D Systems), anti-CD14 (5C5) (Lien *et al.*, 1998) and anti-MD-2 (IIC1). The mouse monoclonal antibody IIC1 (IgM) detects MD-2 in CHO and HEK293 cells expressing TLR4/ MD-2 as well as on the surface of human monocytes (T. Espevik and L. Ryan, unpublished results). Rabbit polyclonal antibodies used: anti-TLR4 (eBioscience), anti-GFP (Clontech) and anti-Hrs (Raiborg *et al.*, 2001). The following mammalian expression vectors were used: pcDNA3 (Invitrogen), CD14 (Latz *et al.*, 2002), *c*-myc-Hrs, *c*-myc-ubiquitin wild type UbRGG (Stang *et al.*, 2004)and *c*-myc-ubiquitin DN UbR (Stang *et al.*, 2004) were in pcDNA3. Dynamin-II wild type and Dynamin-II K44A in pcDNA3 were kindly provided by Dr. Sandy Schmid (Scripps, USA). MD-2 in pEF-BOS was kindly provided by Dr. Miyake (Yang *et al.*, 2000).

Hrs^{YFP} was in pEYFP-C1 (Clontech). The ECFP-2×FYVE construct was made by substituting GFP from EGFP-2×FYVE (Gillooly *et al.*, 2000) with CFP using pECFP (Clontech) as a template and PCR primers 5`CCA AGT ACG CCC CCT ATT GA`3 and 5`ATT TAA GCT TGT ACA GCT CGT CCA TGC`3. The CFP encoding fragment was inserted as a NheI /XhoI fragment.

Cells and cell lines

HEK293 cell lines stably expressed human TLR4 (Yang *et al.*, 2000), $TLR4^{YFP}$, $TLR4^{YFP}$/MD-2 (Latz *et al.*, 2002), or $TLR4^{CFP}$/MD-2 were used and cultured in Dulbecco's modified Eagle's medium (DMEM) supplemented with 10% fetal calf serum (FCS) and 0.5 mg/ml G418 and transfected using GeneJuice^{TM} transfection reagent (Novagene) according to the manufacturer's protocol. Human monocytes were isolated by plastic adherence from Lymphoprep (Axis-Shield) separated buffycoats (The Blood Bank, St Olavs Hospital, Trondheim, Norway) and grown in RPMI/10% pooled A+ serum (The Blood Bank). LPS was sonicated for 5 minutes and preincubated in serum-containing medium at 37°C for 5 min before being added to cells. For confocal imaging the cells were seeded on 35mm glass bottom γ-irradiated tissue cell dishes (MatTek Corporation) and buffered with 25 mM HEPES-buffer just before stimulation. LPS^{CY5} (250 ng/ml) or LPS^{OG} (600 ng/ml) was used in LPS uptake studies.

Flow cytometry

Adherent monocytes were incubated with or without LPS (100 ng/ml) in medium/10% A+ serum for 2 hours, detached with EDTA and stained with 10 µg/ml anti-TLR4 (HTA125) or mouse IgG2a for 30 minutes on ice, washed and incubated

with 10 µg/ml secondary anti-mouse Ig-FITC (Becton Dickinson) for 30 minutes on ice and washed and analyzed by flow cytometry (Coulter).

Short interfering (si)RNA treatment

SiRNA duplexes targeting the coding region of clathrin heavy chain (Motley *et al.*, 2003), the coding region of Hrs (Bache *et al.*, 2003) the coding region of the ESCRT-I component HCRP1 (Bache *et al.*, 2004) were used. A scrambled RNA duplex (Bache *et al.*, 2003) was used as a non-interfering control. All siRNA duplexes used were synthesized by Dharmacon. HEK293 cells and cells expressing $TLR4^{YFP}$/ MD-2 were transfected with 20 nM siRNA for 48 hours using Oligofectamine (Invitrogen) according to the manufacturer's protocol. For the silencing of Hrs and HCRP1 the cells were replated and subjected to a second round of siRNA treatment. For the introduction of plasmid DNA into the siRNA transfected cells, the cells were replated and transfected for 24 hours using the GeneJuice transfection reagent.

Western blotting and immunoprecipitation

HEK293 cells expressing $TLR4^{YFP}$ were plated on 35mm dishes and transfected 24 to 48 hours before 2 washes in PBS and lysed in 100 to 300 µl of lysis buffer (20 mM Tris-HCl, 1 mM EDTA, 1 mM EGTA, 137 mM NaCl, 1% Triton X-100, 1 mM sodium deoxycholate, 10% glycerol, 1 mM Na_3VO_4, 50 mM NaF and Complete protease inhibitor (Roche)). For western blotting the samples were denatured in 1x NuPAGE LDS sample buffer supplemented with 25 mM DTT for 10 min at 70°C. Electrophoresis was performed using NuPAGE novex 7% Tris-Acetate polyacrylamide or 10 % Bis-Tris polyacrylamide gels (Invitrogen) and the samples

blotted onto 0.45 μm nitrocellulose filters (Biorad laboratories) and developed using ECL (Amersham Biosciences). For the analysis of immune complexes, lysates were pre-cleared for 1 hour with protein G sepharose and subsequently incubated for 2 hours with the appropriate antibody (2-3 μg/ml). Immune complexes were harvested with protein G sepharose for 2 hours before 4 washes in lysis buffer. Elution of the immune complexes was performed at 95°C for 10 minutes in 2×LDS sample buffer supplemented with 50 mM DTT.

Confocal imaging

Images of live cells were captured at 37 °C using an Axiovert 100-M microscope with a heated stage equipped with a Zeiss LSM 510 META scanning unit and a 1.4 NA 63x plan apochromat objective. For intracellular staining the cells were permeabilized in 0.05 % saponin, fixed in 3 % paraformalaldehyde and incubated with the appropriate antibody as described previously (Simonsen *et al.*, 1998). For LPS uptake studies in monocytes fluorescently labeled LPS was added to the cells alone or simultaneously with 2 μg/ml Alexa^{546}-labelled anti-TLR4 (HTA125) or 2 μg/ml Alexa546-labelled isotype control. Only ring formed endosomes positive for TLR4 and/or LPS on the limiting membrane (minimal cutoff size 0.5μm) were counted. The total intracellular LPS fluorescence in Fig. 3b was quantified by manually drawing a region of interest that covered the cytoplasm and using the LSM510 software to calculate total fluorescence.

Antigen presentation

The human CD4^{+} Th1 cell clone (T18) specific for mouse antibody constant κ-chain derived peptide Cκ$^{40\text{-}48}$ and restricted by HLA-DR4 (DRA1, B1*0401) was used to

measure T helper cell responses (Schjetne *et al.*, 2003). Antigen presenting cells used were HLA-matched adherent peripheral blood monocytes ($CD14^+$). Tissue culture medium was RPMI 1640 with glucose and L-glutamine (Gibco, Paisley, Scotland) supplemented with pooled 10 % human serum (HS) from blood donors.

Luciferase assay

NFκB activation was determined by a NFκB luciferase reporter assay as described (Latz *et al.*, 2002).

Supplementary data

Supplementary data are available at *The EMBO Journal* Online

Acknowledgement

We thank Liv Ryan for technical assistance. Professor Oddmund Bakke, University of Oslo, generously provided the $EEA1^{CFP}$ construct. This work was supported by The Norwegian Research Council, The Norwegian Cancer Society and the Commission of the European Communities, LSMH-CT-2004-512093, AMIS. Andreas Brech is the recipient of a career scientist fellowship from the FUGE program of the Research Council of Norway. The authors have no conflicting financial interests.

References

Ahmad-Nejad P, Hacker H, Rutz M, Bauer S, Vabulas RM, and Wagner H (2002) Bacterial CpG-DNA and lipopolysaccharides activate Toll-like receptors at distinct cellular compartments. *Eur J Immunol* **32**: 1958-1968

Akira S and Takeda K (2004) Toll-like receptor signalling. *Nat Rev Immunol* **4**: 499-511

Bache KG, Raiborg C, Mehlum A, Madshus IH, and Stenmark H (2002) Phosphorylation of Hrs downstream of the epidermal growth factor receptor. *Eur J Biochem* **269**: 3881-3887

Bache KG, Raiborg C, Mehlum A, and Stenmark H (2003) STAM and Hrs are subunits of a multivalent ubiquitin-binding complex on early endosomes. *J Biol Chem* **278**: 12513-12521

Bache KG, Slagsvold T, Cabezas A, Rosendal KR, Raiborg C, and Stenmark H (2004) The Growth-Regulatory Protein HCRP1/hVps37A Is a Subunit of Mammalian ESCRT-I and Mediates Receptor Down-Regulation. *Mol Biol Cell* **15**: 4337-4346

Boes M, Cerny J, Massol R, Op den Brouw M, Kirchhausen T, Chen J, and Ploegh HL (2002) T-cell engagement of dendritic cells rapidly rearranges MHC class II transport. *Nature* **418**: 983-988

Bonifacino JS and Traub LM (2003) Signals for sorting of transmembrane proteins to endosomes and lysosomes
2. *Annu Rev Biochem* **72**: 395-447

Boone DL, Turer EE, Lee EG, Ahmad RC, Wheeler MT, Tsui C, Hurley P, Chien M, Chai S, Hitotsumatsu O, McNally E, Pickart C, and Ma A (2004) The ubiquitin-modifying enzyme A20 is required for termination of Toll-like receptor responses. *Nat Immunol* **5**: 1052-1060

Chuang TH and Ulevitch RJ (2004) Triad3A, an E3 ubiquitin-protein ligase regulating Toll-like receptors. *Nat Immunol* **5**: 495-502

Damke H, Baba T, Warnock DE, and Schmid SL (1994) Induction of mutant dynamin specifically blocks endocytic coated vesicle formation. *J Cell Biol* **127**: 915-934

Di Guglielmo GM, Le RC, Goodfellow AF, and Wrana JL (2003) Distinct endocytic pathways regulate TGF-beta receptor signalling and turnover. *Nat Cell Biol* **5**: 410-421

Futter CE, Collinson LM, Backer JM, and Hopkins CR (2001) Human VPS34 is required for internal vesicle formation within multivesicular endosomes. *J Cell Biol* **155**: 1251-1264

Gaullier JM, Simonsen A, D'Arrigo A, Bremnes B, Stenmark H, and Aasland R (1998) FYVE fingers bind Ptdins(3)P. *Nature* **394**: 432-433

Gillooly DJ, Morrow IC, Lindsay M, Gould R, Bryant NJ, Gaullier JM, Parton RG, and Stenmark H (2000) Localization of phosphatidylinositol 3-phosphate in yeast and mammalian cells. *EMBO J* **19**: 4577-4588

Gruenberg J and Stenmark H (2004) The biogenesis of multivesicular endosomes. *Nat Rev Mol Cell Biol* **5**: 317-323

Hamerman JA, Tchao NK, Lowell CA, and Lanier LL (2005) Enhanced Toll-like receptor responses in the absence of signaling adaptor DAP12. *Nat Immunol* **6**: 579-586

Hicke L (2001) Protein regulation by monoubiquitin. *Nat Rev Mol Cell Biol* **2**: 195-201

Jackson DC, Lau YF, Le T, Suhrbier A, Deliyannis G, Cheers C, Smith C, Zeng W, and Brown LE (2004) A totally synthetic vaccine of generic structure that targets Toll-like receptor 2 on dendritic

cells and promotes antibody or cytotoxic T cell responses. *Proc Natl Acad Sci U S A* **101**: 15440-15445

Katoh Y, Shiba Y, Mitsuhashi H, Yanagida Y, Takatsu H, and Nakayama K (2004) Tollip and Tom1 form a complex and recruit ubiquitin-conjugated proteins onto early endosomes. *J Biol Chem* **279**: 24435-24443

Kitchens RL, Wang Py, and Munford RS (1998) Bacterial Lipopolysaccharide Can Enter Monocytes Via Two CD14-Dependent Pathways. *J Immunol* **161**: 5534-5545

Komada M and Soriano P (1999) Hrs, a FYVE finger protein localized to early endosomes, is implicated in vesicular traffic and required for ventral folding morphogenesis. *Genes Dev* **13**: 1475-1485

Lamaze C, Dujeancourt A, Baba T, Lo CG, Benmerah A, and utry-Varsat A (2001) Interleukin 2 receptors and detergent-resistant membrane domains define a clathrin-independent endocytic pathway. *Mol Cell* **7**: 661-671

Latz E, Visintin A, Lien E, Fitzgerald KA, Monks BG, Kurt-Jones EA, Golenbock DT, and Espevik T (2002) Lipopolysaccharide rapidly traffics to and from the golgi apparatus with the toll-like receptor 4-MD-2-CD14 complex in a process that is distinct from the initiation of signal transduction. *J Biol Chem* **277**: 47834-47843

Le RC and Wrana JL (2005) Clathrin- and non-clathrin-mediated endocytic regulation of cell signalling. *Nat Rev Mol Cell Biol* **6**: 112-126

Lee Y, Sohn WJ, Kim DS, and Kwon HJ (2004) NF-kappaB- and c-Jun-dependent regulation of human cytomegalovirus immediate-early gene enhancer/promoter in response to lipopolysaccharide and bacterial CpG-oligodeoxynucleotides in macrophage cell line RAW 264.7. *Eur J Biochem* **271**: 1094-1105

Lien E, Aukrust P, Sundan A, Muller F, Froland SS, and Espevik T (1998) Elevated levels of serum-soluble CD14 in human immunodeficiency virus type 1 (HIV-1) infection: Correlation to disease progression and clinical events. *Blood* **92**: 2084-2092

Liew FY, Xu D, Brint EK, and O'Neill LAJ (2005) Negative regulation of toll-like receptor-mediated immune reseponces. *Nat Rev Immunol* **5**: 446-458

Marmor MD and Yarden Y (2004) Role of protein ubiquitylation in regulating endocytosis of receptor tyrosine kinases. *Oncogene* **23**: 2057-2070

Mayor S and Riezman H (2004) Sorting GPI-anchored proteins. *Nat Rev Mol Cell Biol* **5**: 110-120

Mellman I, Fuchs R, and Helenius A (1986) Acidification of the endocytic and exocytic pathways. *Annu Rev Biochem* **55**: 663-700

Motley A, Bright NA, Seaman MNJ, and Robinson MS (2003) Clathrin-mediated endocytosis in AP-2-depleted cells. *J Cell Biol* **162**: 909-918

Nagai Y, Akashi S, Nagafuku M, Ogata M, Iwakura Y, Akira S, Kitamura T, Kosugi A, Kimoto M, and Miyake K (2002) Essential role of MD-2 in LPS responsiveness and TLR4 distribution. *Nat Immunol* **3**: 667-672

Nichols B (2003) Caveosomes and endocytosis of lipid rafts. *J Cell Sci* **116**: 4707-4714

Ohnishi T, Muroi M, and Tanamoto K (2003) MD-2 Is Necessary for the Toll-Like Receptor 4 Protein To Undergo Glycosylation Essential for Its Translocation to the Cell Surface. *Clin Diagn Lab Immunol* **10**: 405-410

Peters PJ, Neefjes JJ, Oorschot V, Ploegh HL, and Geuze HJ (1991) Segregation of Mhc Class-Ii Molecules from Mhc Class-I Molecules in the Golgi-Complex for Transport to Lysosomal Compartments. *Nature* **349**: 669-676

Raiborg C, Bache KG, Gillooly DJ, Madshus IH, Stang E, and Stenmark H (2002) Hrs sorts ubiquitinated proteins into clathrin-coated microdomains of early endosomes. *Nat Cell Biol* **4**: 394-398

Raiborg C, Bache KG, Mehlum A, Stang E, and Stenmark H (2001) Hrs recruits clathrin to early endosomes. *EMBO J* **20**: 5008-5021

Raiborg C, Rusten TE, and Stenmark H (2003) Protein sorting into multivesicular endosomes. *Curr Opin Cell Biol* **15**: 446-455

Schjetne KW, Thompson KM, Nilsen N, Flo TH, Fleckenstein B, Iversen JG, Espevik T, and Bogen B (2003) Cutting edge: link between innate and adaptive immunity: Toll-like receptor 2 internalizes antigen for presentation to CD4+ T cells and could be an efficient vaccine target. *J Immunol* **171**: 32-36

Schjetne KW, Thompson KM, Aarvak T, Fleckenstein B, Sollid LM, and Bogen B (2002) A mouse C{kappa}-specific T cell clone indicates that DC-SIGN is an efficient target for antibody-mediated delivery of T cell epitopes for MHC class II presentation. *Int Immunol* **14**: 1423-1430

Scoles DR, Qin Y, Nguyen V, Gutmann DH, and Pulst SM (2005) HRS inhibits EGF receptor signaling in the RT4 rat schwannoma cell line. *Biochem Biophys Res Commun* **335**: 385-392

Shimazu R, Akashi S, Ogata H, Nagai Y, Fukudome K, Miyake K, and Kimoto M (1999) MD-2, a Molecule that Confers Lipopolysaccharide Responsiveness on Toll-like Receptor 4á. *J Exp Med* **189**: 1777-1782

Sigismund S, Woelk T, Puri C, Maspero E, Tacchetti C, Transidico P, Di Fiore PP, and Polo S (2005) Clathrin-independent endocytosis of ubiquitinated cargos. *Proc Natl Acad Sci U S A* **102**: 2760-2765

Simonsen A, Lippe R, Christoforidis S, Gaullier JM, Brech A, Callaghan J, Toh BH, Murphy C, Zerial M, and Stenmark H (1998) EEA1 links PI(3)K function to Rab5 regulation of endosome fusion. *Nature* **394**: 494-498

Stang E, Blystad FD, Kazazic M, Bertelsen V, Brodahl T, Raiborg C, Stenmark H, and Madshus IH (2004) Cbl-dependent ubiquitination is required for progression of EGF receptors into clathrin-coated pits. *Mol Biol Cell* **15**: 3591-3604

Stenmark H, Aasland R, Toh BH, and D'Arrigo A (1996) Endosomal localization of the autoantigen EEA1 is mediated by a zinc-binding FYVE finger. *J Biol Chem* **271**: 24048-24054

Thieblemont N and Wright SD (1999) Transport of Bacterial Lipopolysaccharide to the Golgi Apparatus. *J Exp Med* **190**: 523-534

Triantafilou M, Morath S, Mackie A, Hartung T, and Triantafilou K (2004) Lateral diffusion of Toll-like receptors reveals that they are transiently confined within lipid rafts on the plasma membrane. *J Cell Sci* **117**: 4007-4014

Urbe S, Mills IG, Stenmark H, Kitamura N, and Clague MJ (2000) Endosomal Localization and Receptor Dynamics Determine Tyrosine Phosphorylation of Hepatocyte Growth Factor-Regulated Tyrosine Kinase Substrate. *Mol Cell Biol* **20**: 7685-7692

Vieira OV, Harrison RE, Scott CC, Stenmark H, Alexander D, Liu J, Gruenberg J, Schreiber AD, and Grinstein S (2004) Acquisition of Hrs, an Essential Component of Phagosomal Maturation, Is Impaired by Mycobacteria. *Mol Cell Biol* **24**: 4593-4604

Waage A, Brandtzaeg P, Halstensen A, Kierulf P, and Espevik T (1989) The complex pattern of cytokines in serum from patients with meningococcal septic shock. Association between interleukin 6, interleukin 1, and fatal outcome. *J Exp Med* **169**: 333-338

Yang H, Young DW, Gusovsky F, and Chow JC (2000) Cellular Events Mediated by Lipopolysaccharide-stimulated Toll-like Receptor 4. MD-2 is required for activation of mitogen-activated protein kinase and Elk-1. *J Biol Chem* **275**: 20861-20866

Zhang G and Ghosh S (2002) Negative regulation of toll-like receptor-mediated signaling by Tollip. *J Biol Chem* **277**: 7059-7065

Figure legends

Figure 1. The LPS receptor complex is endocytosed and appears on endosomal structures in human monocytes. (**a**) Flow cytometry showing downregulation of surface TLR4. The surface TLR4 level was monitored in monocytes before and after LPS (2 ng/ml) stimulation using the TLR4 antibody HTA125 and the mouse IgG2a as a isotype control (**b**) Confocal images of monocytes stimulated with Cy5-labelled LPS (LPS^{CY5}). The monocytes were incubated with LPS^{Cy5} (250 ng/ml) and monitored over a period of 5 hours. Arrows indicate LPS positive endosomal structures. (**c**) Confocal images of monocytes stimulated with OregonGreen-labeled LPS (LPS^{OG}) and co-incubated with Alexa546-labelled HTA125 (anti-$TLR4^{A546}$). Images were captured 1 hour after addition of anti-$TLR4^{A546}$ (2 µg/ml) and LPS^{OG} (600 ng/ml). No uptake was observed for the Alexa546 labeled mouse isotype control IgG2a (2 µg/ml) (data not shown). Bar = 5 µm.

Figure 2. LPS is internalized on early endosomes containing TLR4. HEK293 cells expressing $TLR4^{YFP}$/MD-2 or $TLR4^{YFP}$ only, were transfected with CD14 and stimulated by adding LPS^{Cy5} (250 ng/ml). (**a**) Confocal images before (left) and 30 minutes after (right) the addition of LPS^{Cy5}. (**b**) Estimation of the number $TLR4^{YFP}$-containing endosomes (>0.5µm) before and after stimulation. The $TLR4^{YFP}$-containing endosomes were counted in living cells without stimulation and in the period 10 to 40 minutes after LPS^{Cy5} stimulation. The number of cells analyzed were n=52 cells for each situation. (**c**) Comparison of the number of $TLR4^{YFP}$-containing endosomes (>0.5µm) with and without co-expression of MD-2. The LPS positive endosomes with TLR4 co-localization was quantified as above in CD14 transfected cells expressing $TLR4^{YFP}$/MD-2 (n=85) or cells expressing $TLR4^{YFP}$ (n=103). (**d**)

Confocal images of cells showing co-localization of TLR4 and LPS on early/sorting endosomes. HEK293 cells expressing $TLR4^{YFP}$/MD-2 co-transfected with CD14 and the marker for early/sorting endosomes, $2\times FYVE^{CFP}$, 45 minutes after the addition of LPS^{Cy5}. (**e**) Confocal image of a cell transfected as in (d) and simultaneously given $Alexa^{546}$-labeled transferrin Tf^{A546} (5µg/ml) and LPS^{Cy5}. Full sized images of each the four channels of the overlaid image are shown in Supplementary Figure 2. All the images presented in this figure represent optical sections of 1.3 µm and one individual scan per cell was used for the counting of TLR4 positive endosomes. Bar=5 µm.

Figure 3. Endocytosis of the LPS receptor complex is dependent on dynamin and clathrin. (**a**) Confocal images of dynamin WT (left) and Dyn K44A (right) transfected cells. HEK293 cells expressing $TLR4^{YFP}$/MD-2 were transfected with CD14 together with dynamin WT or Dyn K44A and left for 6 days before analysis. The cells were simultaneously given LPS^{Cy5} (250 ng/ml) and $Alexa^{546}$-labeled transferrin (Tf^{A546}) (5µg/ml) and imaged after 50 minutes. (**b**) Comparison of the total LPS uptake in dynamin WT (n=46) and Dyn K44A (n=52) transfected cells in fixed cells 75 minutes after LPS^{Cy5} stimulation. The LPS uptake was quantified using the LSM510 software by measuring total intracellular fluorescence in manually drawn regions of interest and the number of cells analysed were n=46 for the dynamin WT and n=52 for the Dyn K44A transfectants. (**c**) Confocal images of control siRNA treated cells (left) and clathrin siRNA treated cells (right) following LPS^{Cy5} stimulation. HEK293 cells expressing $TLR4^{YFP}$/MD-2 were treated with control or clathrin siRNA for 48 hours followed by a 24 hours transfection with CD14. The cells were simultaneously given LPS^{Cy5} (250 ng/ml) and Tf^{A546} (5µg/ml) and imaged after 35 minutes. (**d**) Comparison of the number of LPS positive endosomes (>0.5 µm) per cell in cells transfected with

control siRNA and clathrin siRNA 10 to 40 min after LPS^{Cy5} stimulation. The number of cells monitored was n=33 (control siRNA) and n=25 (clathrin siRNA). Clathrin- and control siRNA-treated HEK293 cells transfected with CD14 alone were included for comparison (n=40 and 16, respectively). Bar = 10 µm.

Figure 4. LPS promotes TLR4 ubiquitination and the association of TLR4 with Hrs. (**a**) HEK293 cells expressing $TLR4^{YFP}$/MD-2 were stimulated with LPS (1µg/ml) for indicated time periods. $TLR4^{YFP}$ was immuno-precipitated with a polyclonal anti-GFP antibody and blotted for ubiquitin (FK2 antibody) and GFP (monoclonal GFP antibody). (**b**) Monocytes were either left untreated or stimulated with LPS (1 µg/ml) for indicated time periods. Cellular lysates were made and TLR4 immuno-precipitated with a polyclonal TLR4 antibody and blotted for ubiquitin (left), TLR4 (middle) and Hrs (lower left) or the reverse immunoprecipitatation of Hrs or control IgG blotted for TLR4 (upper right). The Hrs in lysate is shown in the lower rigth panel.(**c**) HEK293 cells expressing $TLR4^{YFP}$/MD-2 were transfected with *c*-myc-tagged Hrs for 24 hours before LPS stimulation for indicated periods. Cellular lysates were prepared and immuno-precipitated with anti-GFP ($TLR4^{YFP}$) or control IgG (C1) and blotted for Hrs. Control C2 represents Hrs immunoprecipitated from non-transfected HEK293 cells showing the size of endogenous Hrs. Overexpression of Hrs resulted in a LPS-induced reduction in TLR4 levels in lysates whereas Hrs and tubulin levels are unaffected (lower three panels). (**d**) Confocal images of HEK293 cells expressing $TLR4^{CFP}$/MD-2 transfected with CD14 and Hrs^{YFP} following 3 hours of LPS (250 ng/ml) stimulation. Bar=5µm.

Figure 5. Lysosomal degradation of TLR4 limits signaling. (**a**) HEK293 cells expressing TLR4YFP/MD-2 were transfected with CD14 and treated with chloroquine (10 μM) or lactacystin (10μM) for 30 minutes prior LPS (1μg/ml) stimulation for indicated time periods. Cellular lysates were made and $TLR4^{YFP}$ detected using a polyclonal anti-GFP antibody and reblotted for α-tubulin as a control for equal loading. The samples displayed represent sections of the original blot. (**b**) HEK293 cells expressing $TLR4^{YFP}$/MD-2 were transfected with CD14 and treated with 10 μM LY or control vehicle (EtOH) for 30 minutes and stimulated with LPS (1μg/ml) for 10 hours. Cellular lysates were made and $TLR4^{YFP}$ detected using a polyclonal anti-GFP antibody a reblotted for α-tubulin as a control for equal loading. (**c**) HEK293 cells expressing $TLR4^{YFP}$/MD-2 were treated with control of Hrs siRNA and transfected with CD14. Cellular lysates were made and blotted for GFP ($TLR4^{YFP}$), Hrs, and α-tubulin for the examination of $TLR4^{YFP}$ and Hrs levels. The samples displayed represent sections of the original blot. (**d**) Effect of dynamin and ubiquitination on LPS induced NFκB activation through TLR4. HEK293 cells expressing TLR4 were transfected with MD-2, CD14 and Elam-luc together with WT constructs (dynamin and UbRGG) or a dominant negative version of dynamin (Dyn K44A) or an inhibitory version of ubiquitin (UbR, lacking the two C-terminal glycines necessary for conjugation to proteins but able to occupy ubiquitin binding pockets). The cells were stimulated for 6 hours with LPS (10 ng/ml) and assayed for NFκB-induced luciferase expression. (**e**) Effect of Hrs and ESCRT-I on LPS induced NFκB activation through TLR4. HEK293 cells expressing $TLR4^{YFP}$/MD-2 were treated with control siRNA or siRNA directed towards Hrs, or HCRP1 (component of ESCRT-I) and co-transfected with CD14 and Elam-luc as described in the materials and methods section and assayed for NFκB-induced luciferase expression.

Figure 6. The LPS receptor complex is trafficked to the classII loading compartment. (**a**) Confocal images showing $TLR4^{YFP}$ in the lumen of LAMP-1 positive endosomes. HEK293 cells expressing $TLR4^{YFP}$/MD-2 transfected with CD14 were treated for 2 hours with LPS (1μg/ml) and fixed before intracellular staining for LAMP1. Arrows indicate LAMP-1 positive endosomes showing intraluminal $TLR4^{YFP}$ (**b**) Confocal images showing $TLR4^{YFP}$ in the lumen of non-acidic endosomes. HEK293 cells expressing $TLR4^{YFP}$/MD-2 transfected with CD14 were stimulated with LPS (1μg/ml) for 3 hours and incubated with 10 nM LysoTracker Red (**c**). Antibodies towards TLR4 (HTA125), CD14 (5C5) or MD-2 (IIC1) or isotype matched controls were added to human HLA-matched monocytes together with cloned DR4-restricted $CD4^+$ T cells specific for mouse $C\kappa^{40-48}$. T cell proliferation was measured after 48 hours by incorporation of $[^3H]$ TdR. Data points are mean of duplicates from a representative experiment. Isotype-matched monoclonal antibodies were used as controls. Bar=5 μm.

Figure legends

Figure 1. The LPS receptor complex is endocytosed and appears on endosomal structures in human monocytes. (**a**) Flow cytometry showing downregulation of surface TLR4. The surface TLR4 level was monitored in monocytes before and after LPS (2 ng/ml) stimulation using the TLR4 antibody HTA125 and the mouse IgG2a as a isotype control (**b**) Confocal images of monocytes stimulated with Cy5-labelled LPS (LPS^{CY5}). The monocytes were incubated with LPS^{Cy5} (250 ng/ml) and monitored over a period of 5 hours. Arrows indicate LPS positive endosomal structures. (**c**) Confocal images of monocytes stimulated with OregonGreen-labeled LPS (LPS^{OG}) and co-incubated with Alexa546-labelled HTA125 (anti-$TLR4^{A546}$). Images were captured 1 hour after addition of anti-$TLR4^{A546}$ (2 µg/ml) and LPS^{OG} (600 ng/ml). No uptake was observed for the Alexa546 labeled mouse isotype control IgG2a (2 µg/ml) (data not shown). Bar = 5 µm.

Figure 2. LPS is internalized on early endosomes containing TLR4. HEK293 cells stably expressing $TLR4^{YFP}$/MD-2 or $TLR4^{YFP}$ only were transfected with CD14 and stimulated by adding LPS^{Cy5} (250 ng/ml). (**a**) Confocal images before (left) and 30 minutes after (right) the addition of LPS^{Cy5}. (**b**) Estimation of the number $TLR4^{YFP}$-containing endosomes (>0.5µm) before and after stimulation. The $TLR4^{YFP}$-containing endosomes were counted in living cells without stimulation and in the period 10 to 40 minutes after LPS^{Cy5} stimulation. The number of cells analysed were n=52 cells for each situation. (**c**) Comparison of the number of $TLR4^{YFP}$-containing endosomes (>0.5µm) with and without co-expression of MD-2. The LPS positive endosomes with TLR4 co-localization was quantified as above in CD14 transfected cells expressing $TLR4^{YFP}$/MD-2 (n=85) or cells expressing $TLR4^{YFP}$ (n=103). (**d**)

Confocal images of cells showing co-localization of TLR4 and LPS on early/sorting endosomes. HEK293 cells expressing $TLR4^{YFP}$/MD-2 co-transfected with CD14 and the marker for early/sorting endosomes, $2\times FYVE^{CFP}$, 45 minutes after the addition of LPS^{Cy5}. (**e**) Confocal image of a cell transfected as in (d) and simultaneously given $Alexa^{546}$-labeled transferrin Tf^{A546} (5µg/ml) and LPS^{Cy5}. Full sized images of each the four channels of the overlaid image are shown in Supplementary Figure 2. All the images presented in this figure represent optical sections of 1.3 µm and one individual scan per cell was used for the counting of TLR4 positive endosomes. Bar=5 µm.

Figure 3. Endocytosis of the LPS receptor complex is dependent on dynamin and clathrin. (**a**) Confocal images of dynamin WT (left) and Dyn K44A (right) transfected cells. HEK293 cells expressing $TLR4^{YFP}$/MD-2 were transfected with CD14 together with dynamin WT or Dyn K44A and left for 6 days before analysis. The cells were simultaneously given LPS^{Cy5} (250 ng/ml) and $Alexa^{546}$-labeled transferrin (Tf^{A546}) (5µg/ml) and imaged after 50 minutes. (**b**) Comparison of the total LPS uptake in dynamin WT (n=46) and Dyn K44A (n=52) transfected cells in fixed cells 75 minutes after LPS^{Cy5} stimulation. The LPS uptake was quantified using the LSM510 software by measuring total intracellular fluorescence in manually drawn regions of interest and the number of cells analysed were n=46 for the dynamin WT and n=52 for the Dyn K44A transfectants. (**c**) Confocal images of control siRNA treated cells (left) and clathrin siRNA treated cells (right) following LPS^{Cy5} stimulation. HEK293 cells expressing $TLR4^{YFP}$/MD-2 were treated with control or clathrin siRNA for 48 hours followed by a 24 hours transfection with CD14. The cells were simultaneously given LPS^{Cy5} (250 ng/ml) and Tf^{A546} (5µg/ml) and imaged after 35 minutes. (**d**) Comparison of the number of LPS positive endosomes (>0.5 µm) per cell in cells transfected with

control siRNA and clathrin siRNA 10 to 40 min after LPS^{Cy5} stimulation. The number of cells monitored was n=33 (control siRNA) and n=25 (clathrin siRNA). Clathrin- and control siRNA-treated HEK293 cells transfected with CD14 alone were included for comparison (n=40 and 16, respectively). Bar = 10 µm.

Figure 4. LPS promotes TLR4 ubiquitination and the association of TLR4 with Hrs. (**a**) HEK293 cells expressing $TLR4^{YFP}$/MD-2 were stimulated with LPS (1µg/ml) for indicated time periods. $TLR4^{YFP}$ was immuno-precipitated with a polyclonal anti-GFP antibody and blotted for ubiquitin (FK2 antibody) and GFP (monoclonal GFP antibody). (**b**) Monocytes were either left untreated or stimulated with LPS (1 µg/ml) for indicated time periods. Cellular lysates were made and TLR4 immuno-precipitated with a polyclonal TLR4 antibody and blotted for ubiquitin (left), TLR4 (middle) and Hrs (lower left) or the reverse immunoprecipitatation of Hrs or control IgG blotted for TLR4 (upper right). The Hrs in lysate is shown in the lower rigth panel.(**c**) HEK293 cells expressing $TLR4^{YFP}$/MD-2 were transfected with *c*-myc-tagged Hrs for 24 hours before LPS stimulation for indicated periods. Cellular lysates were prepared and immuno-precipitated with anti_GFP ($TLR4^{YFP}$) or control IgG (C1) and blotted for Hrs. Control C2 represents Hrs immunoprecipitated from non-trasfected HEK293 cells showing the size of endogenous Hrs. Overexpression of Hrs resulted in a LPS-induced reduction in TLR4 levels in lysates whereas Hrs and tubulin levels are unaffected (lower three panels). (**d**) Confocal images of HEK293 cells expressing $TLR4^{CFP}$/MD-2 transfected with CD14 and Hrs^{YFP} following 3 hours of LPS (250 ng/ml) stimulation. Bar=5µm.

Figure 5. Lysosomal degradation of TLR4 limits signaling. (**a**) HEK293 cells expressing TLR4YFP/MD-2 were transfected with CD14 and treated with chloroquine (10 μM) or lactacystin (10μM) for 30 minutes prior LPS (1μg/ml) stimulation for indicated time periods. Cellular lysates were made and $TLR4^{YFP}$ detected using a polyclonal anti-GFP antibody. The filter was reblotted for α-tubulin as a control for equal loading. The samples displayed represent sections of the original blot. (**b**) HEK293 cells expressing TLR4YFP/MD-2 were transfected with CD14 and treated with 10 μM LY or control vehicle (EtOH) for 30 minutes and stimulated with LPS (1μg/ml) for 10 hours. Cellular lysates were made and $TLR4^{YFP}$ detected using a polyclonal anti-GFP antibody. The filter was reblotted for α-tubulin as a control for equal loading. (**c**) HEK293 cells expressing $TLR4^{YFP}$/MD-2 were treated with control of Hrs siRNA and transfected with CD14. The cells were lysed and blotted for GFP ($TLR4^{YFP}$), Hrs, and α-tubulin for the examination of $TLR4^{YFP}$ and Hrs levels. The samples displayed represent sections of the original blot. (**d**) Effect of dynamin and ubiquitination on LPS induced NFκB activation through TLR4. HEK293 cells expressing TLR4 were transfected with MD-2, CD14 and Elam-luc together with WT constructs (dynamin and UbRGG) or a dominant negative version of dynamin (Dyn K44A) or an inhibitory version of ubiquitin (UbR, lacking the two C-terminal glycines necessary for conjugation to proteins but able to occupy ubiquitin binding pockets). The cells were stimulated for 6 hours with LPS (10 ng/ml) and assayed for NFκB-induced luciferase expression. (**e**) Effect of Hrs and ESCRT-I on LPS induced NFκB activation through TLR4. HEK293 cells expressing $TLR4^{YFP}$/MD-2 were treated with control siRNA or siRNA directed towards Hrs, or HCRP1 (component of ESCRT-I) and co-transfected with CD14 and Elam-luc as described in the materials and methods section and assayed for NFκB-induced luciferase expression.

Figure 6. The LPS receptor complex is trafficked to the class II loading compartment. (**a**) Confocal images showing $TLR4^{YFP}$ in the lumen of LAMP-1 positive endosomes. HEK293 cells expressing $TLR4^{YFP}$/MD-2 transfected with CD14 were treated for 2 hours with LPS (1μg/ml) and fixed before intracellular staining for LAMP1. Arrows indicate LAMP-1 positive endosomes showing intraluminal $TLR4^{YFP}$ (**b**) Confocal images showing $TLR4^{YFP}$ in the lumen of non-acidic endosomes. HEK293 cells expressing $TLR4^{YFP}$/MD-2 transfected with CD14 were stimulated with LPS (1μg/ml) for 3 hours and incubated with 10 nM LysoTracker Red (**c**). Antibodies towards TLR4 (HTA125), CD14 (5C5) or MD-2 (IIC1) or isotype matched controls were added to human HLA-matched monocytes together with cloned DR4-restricted $CD4^+$ T cells specific for mouse $C\kappa^{40-48}$. T cell proliferation was measured after 48 hours by incorporation of $[^3H]$ TdR. Data points are mean of duplicates (background subtracted) from a representative experiment. Isotype-matched mAbs were used as controls. Bar=5 μm.

Figure 1

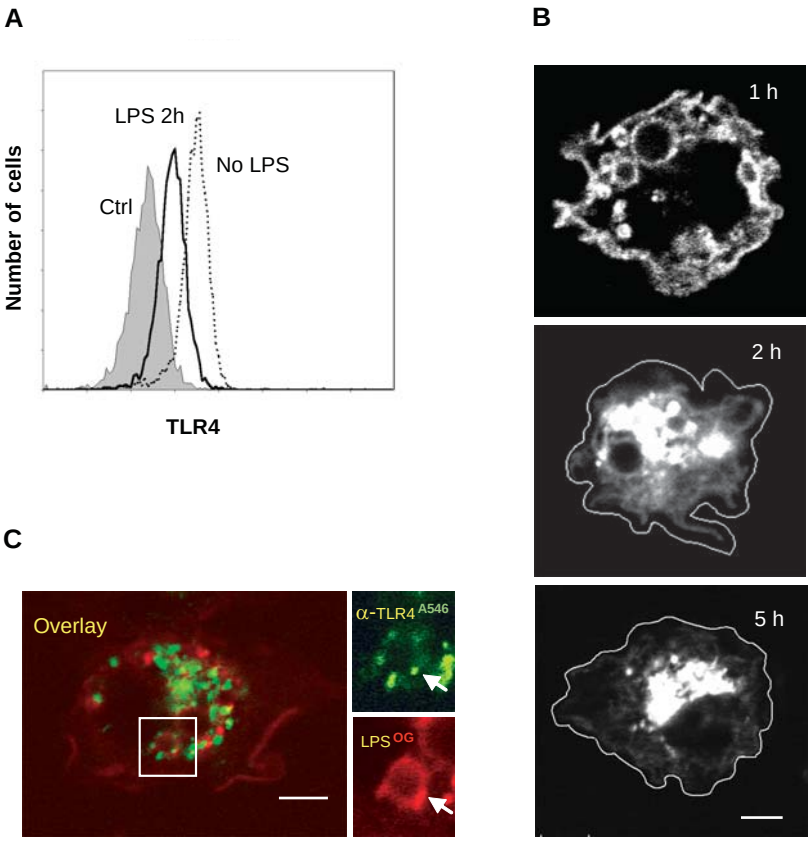
A
LPS 2h
No LPS
Ctrl
Number of cells
TLR4
B
1 h
2 h
5 h
C
Overlay
α-TLR4 A546
LPS OG

Figure 2

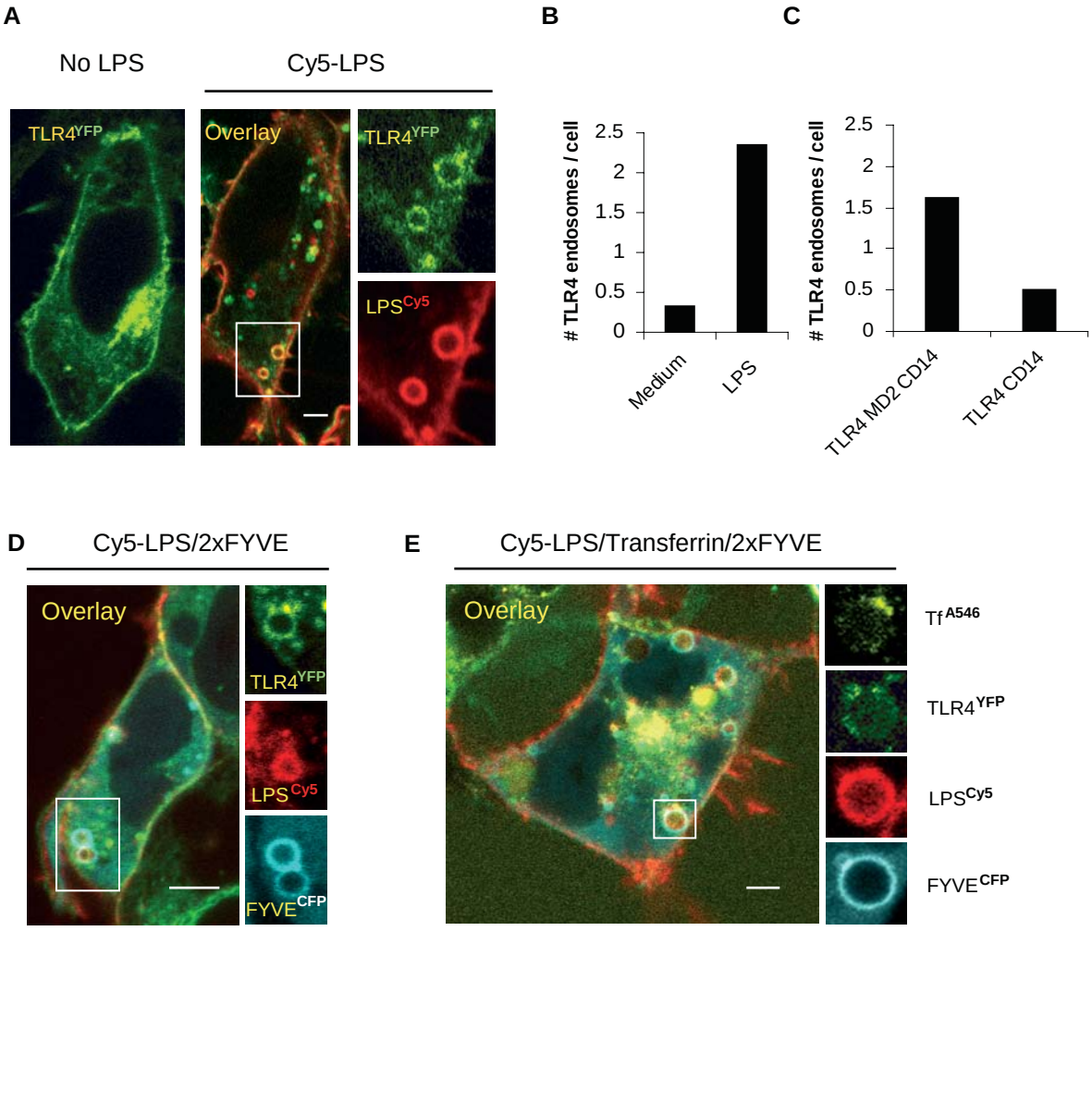
A
No LPS
Cy5-LPS
TLR4YFP
Overlay
TLR4YFP
LPSCy5
B
TLR4 endosomes / cell
2.5
2
1.5
1
0.5
0
Medium
LPS
C
TLR4 endosomes / cell
2.5
2
1.5
1
0.5
0
TLR4 MD2 CD14
TLR4 CD14
D
Cy5-LPS/2xFYVE
Overlay
TLR4YFP
LPSCy5
FYVECFP
E
Cy5-LPS/Transferrin/2xFYVE
Overlay
TfA546
TLR4YFP
LPSCy5
FYVECFP

Figure 3

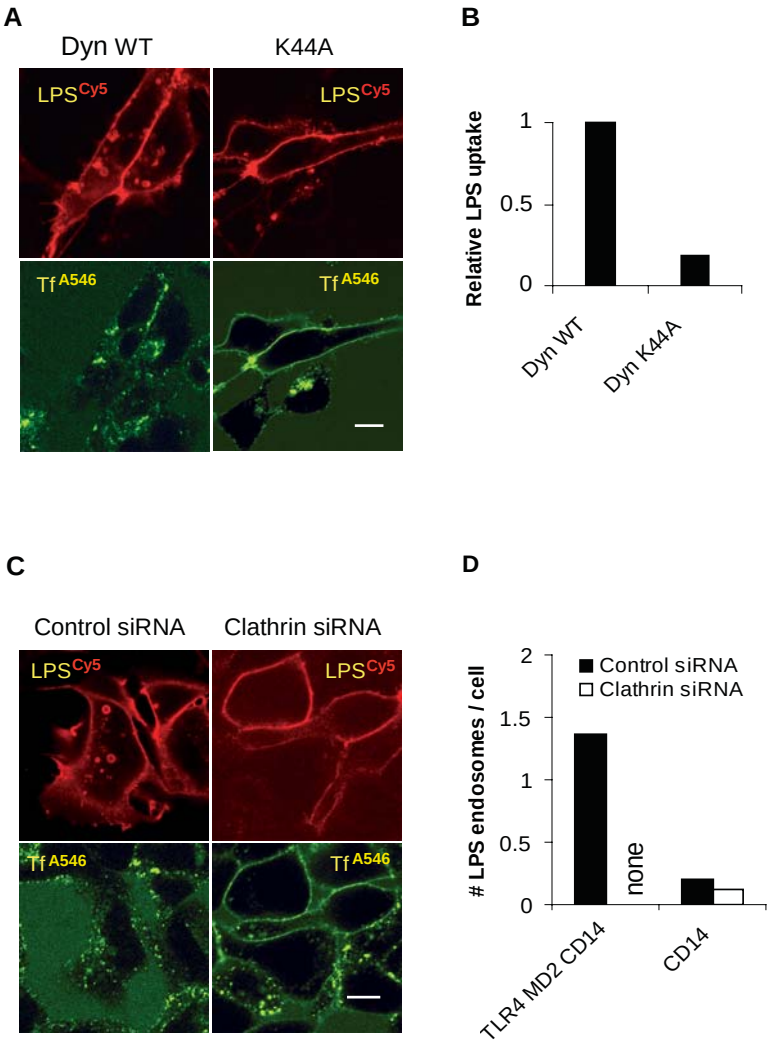
A
Dyn WT
K44A
LPS Cy5
LPS Cy5
Tf A546
Tf A546
B
Relative LPS uptake
1
0.5
0
Dyn WT
Dyn K44A
C
Control siRNA
Clathrin siRNA
LPS Cy5
LPS Cy5
Tf A546
Tf A546
D
LPS endosomes / cell
2
1.5
1
0.5
0
Control siRNA
Clathrin siRNA
none
TLR4 MD2 CD14
CD14

Figure 4

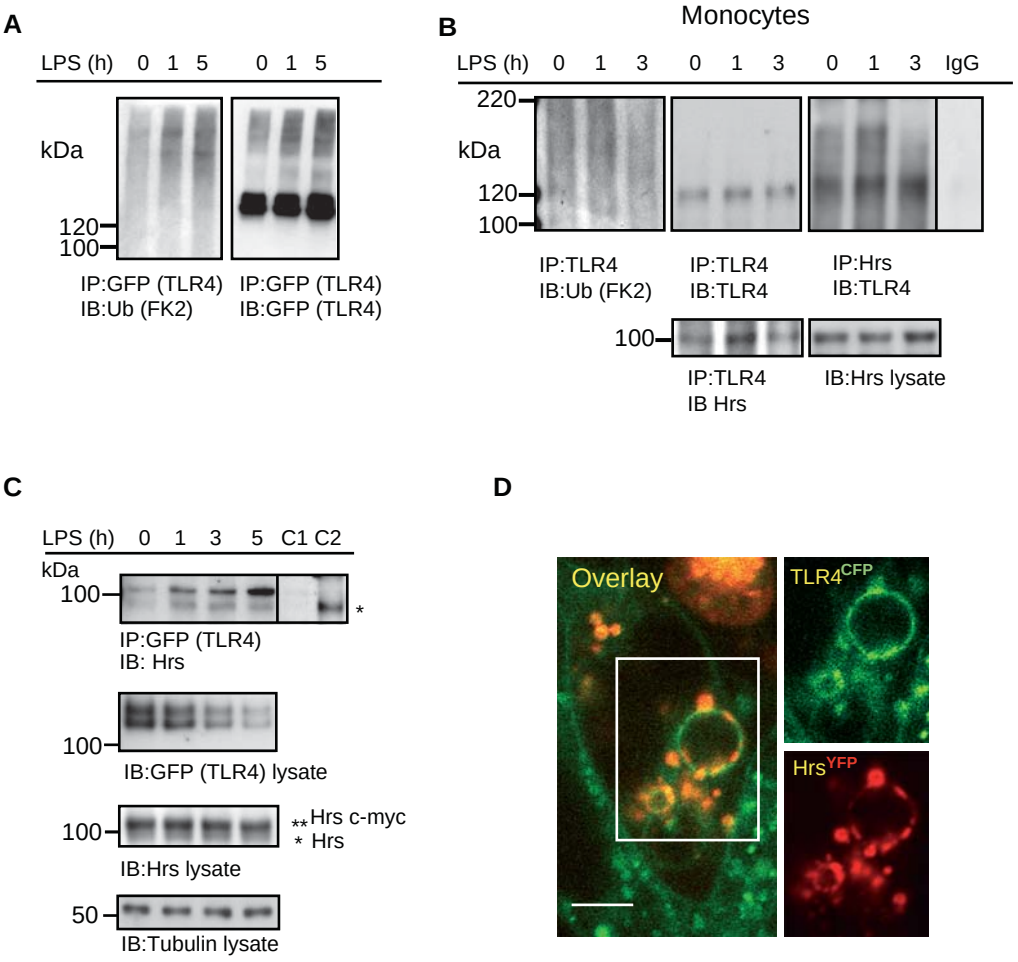
A
LPS (h) 0 1 5 0 1 5
kDa
120
100
IP:GFP (TLR4)
IB:Ub (FK2)
IP:GFP (TLR4)
IB:GFP (TLR4)
B
Monocytes
LPS (h) 0 1 3 0 1 3 0 1 3 IgG
220
kDa
120
100
IP:TLR4
IB:Ub (FK2)
IP:TLR4
IB:TLR4
IP:Hrs
IB:TLR4
100
IP:TLR4
IB Hrs
IB:Hrs lysate
C
LPS (h) 0 1 3 5 C1 C2
kDa
100
*
IP:GFP (TLR4)
IB: Hrs
100
IB:GFP (TLR4) lysate
100
** Hrs c-myc
* Hrs
IB:Hrs lysate
50
IB:Tubulin lysate
D
Overlay
TLR4CFP
HrsYFP

Figure 5

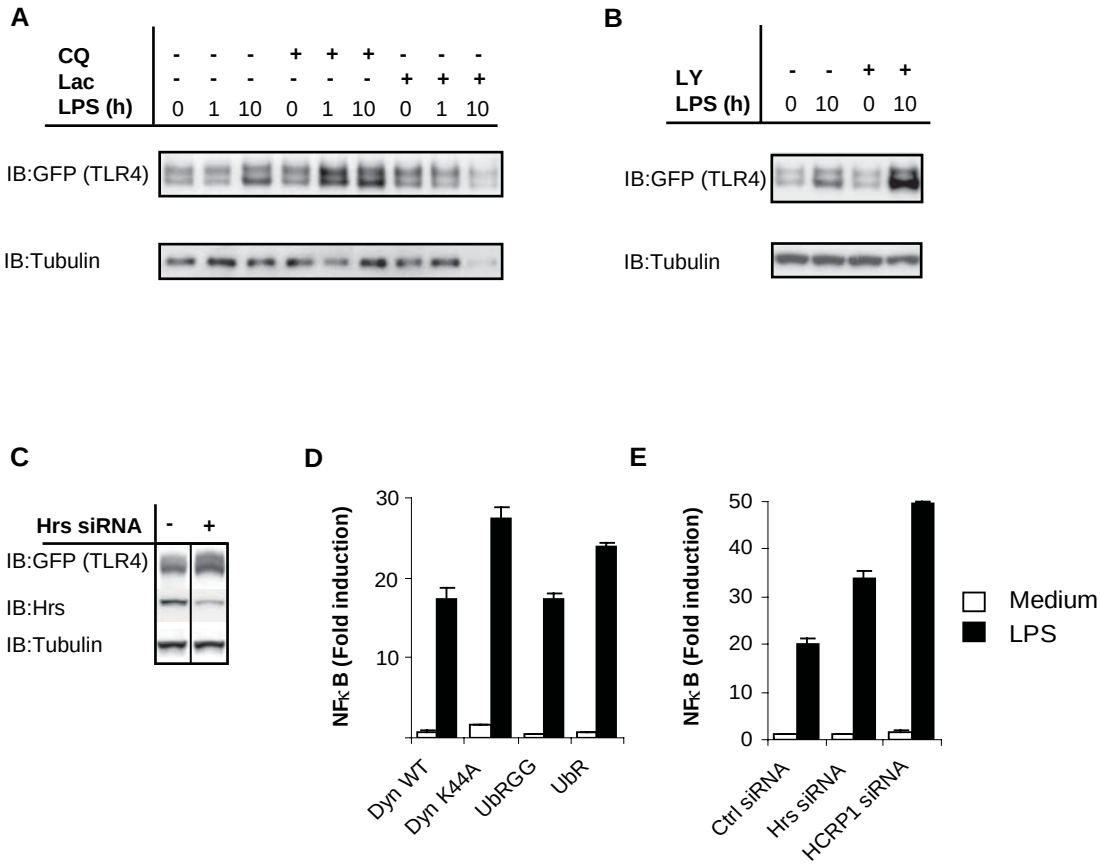
A
CQ
Lac
LPS (h)
0 1 10 0 1 10 0 1 10
IB:GFP (TLR4)
IB:Tubulin
B
LY
LPS (h)
0 10 0 10
IB:GFP (TLR4)
IB:Tubulin
C
Hrs siRNA
IB:GFP (TLR4)
IB:Hrs
IB:Tubulin
D
NFκB (Fold induction)
Dyn WT
Dyn K44A
UbRGG
UbR
E
NFκB (Fold induction)
Ctrl siRNA
Hrs siRNA
HCRP1 siRNA
Medium
LPS

Figure 6

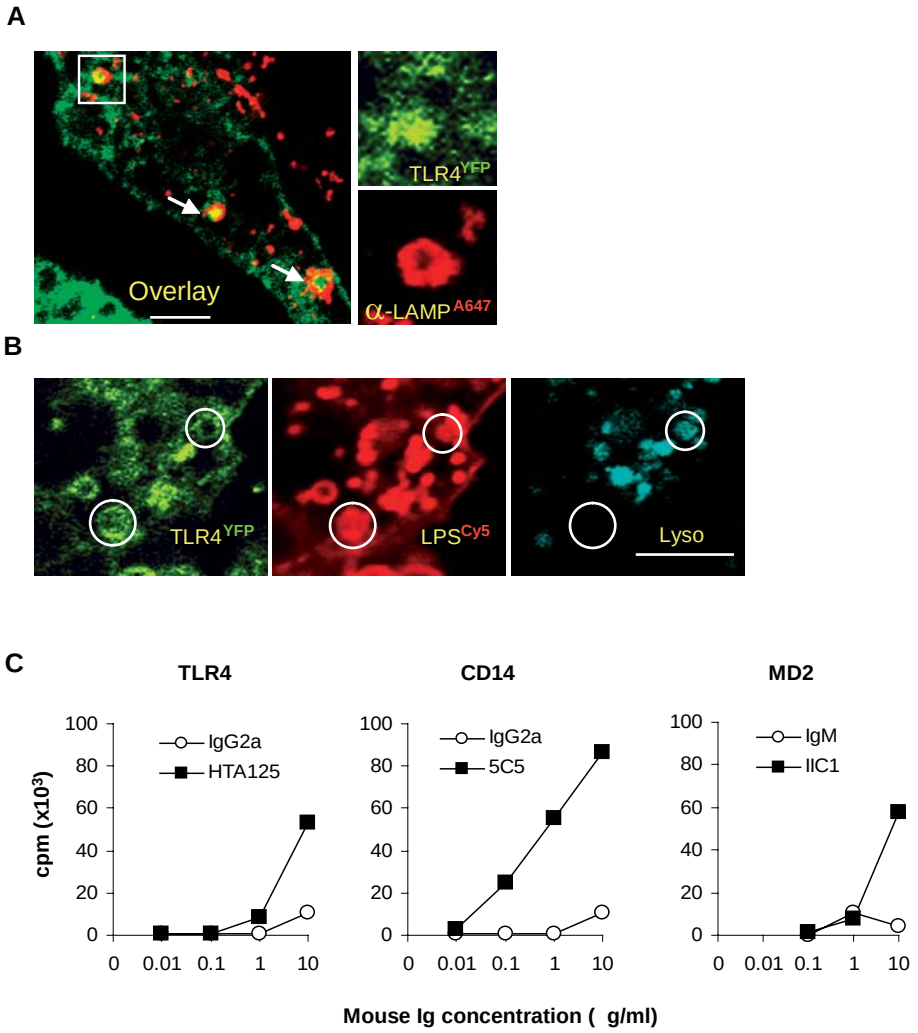
A
Overlay
TLR4YFP
α-LAMPA647
B
TLR4YFP
LPSCy5
Lyso
C
TLR4
CD14
MD2
IgG2a
HTA125
5C5
IgM
IIC1
cpm (x10³)
100
80
60
40
20
0
0 0.01 0.1 1 10
Mouse Ig concentration (g/ml)

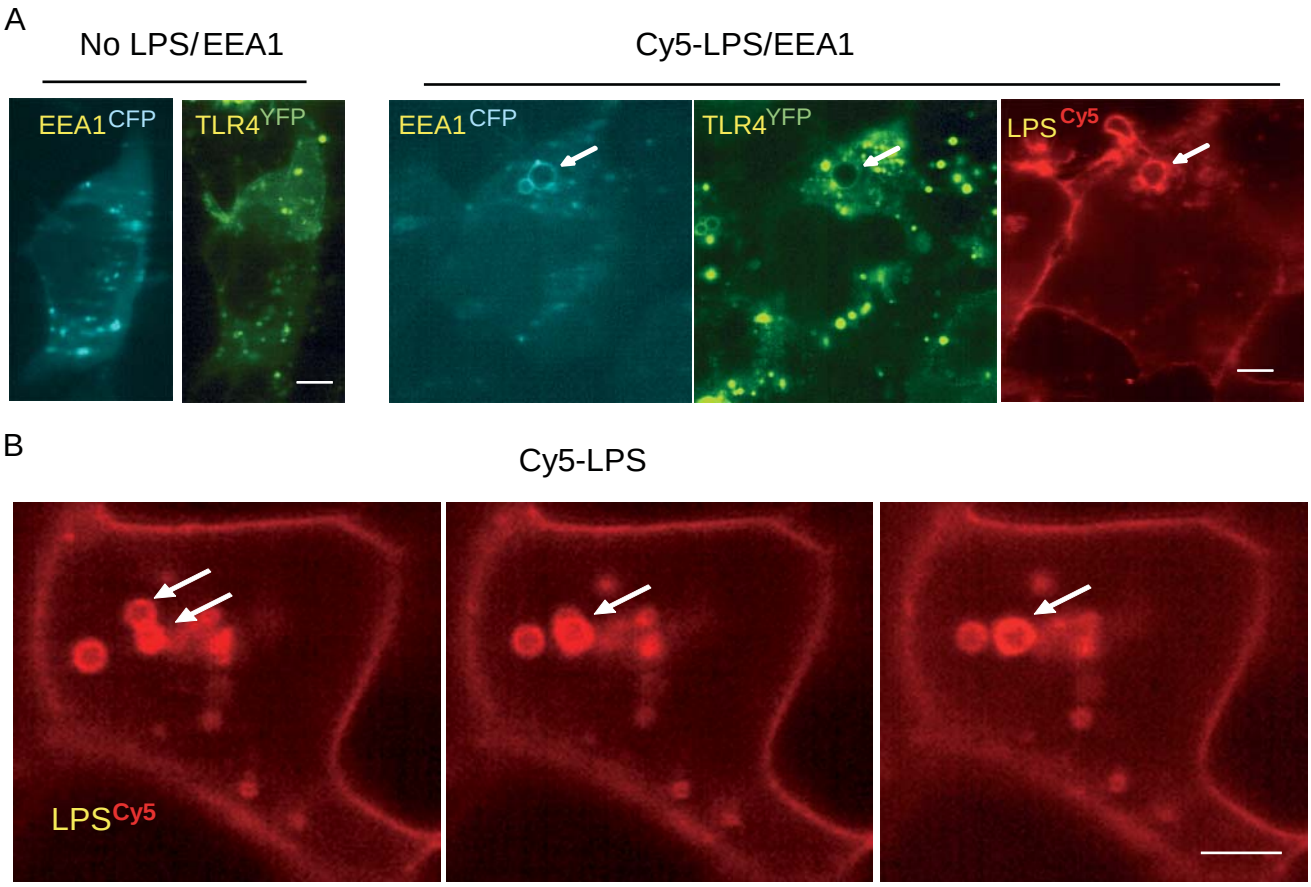

Supplementary Information, Figure 1.
Addition of LPS results in enlarged early/sorting endosomes.
HEK293 cells stably expressing $TLR4^{YFP}$ and MD-2 were transfected with CD14 and $EEA1^{CFP}$ (A), and stimulated by adding LPS^{Cy5} (250 ng/ml). The left panel shows the confocal images of a cell without stimulation and the rigth panel a cell after 30 minutes of LPS^{Cy5} stimulation. Enlarged EEA1 positive endosomes (arrow) were not observed in unstimulated cells. HEK293 cells stably expressing TLR4YFP/MD-2 were transfected with CD14 and incubated with LPS^{Cy5}(B). LPS positive endosomes engaged in a fusion event are shown (arrows). The fusion of the two equally sized large LPS positive endosomes gives rise to an endosome with a 25% increased diameter. Time interval between each image capture is 5 s. These three images are taken from the Supplementary Movie 1. Bar = 5µm

Methods: LPS (0111:B4) from Escherichia coli was purchased from Invivogen. Cy5-labelling of LPS was performed as previously described (Latz et al., 2002). The EEA1 in pECFP-C1 (Clontech) ($EEA1^{CFP}$) encodes the C-terminal part of EEA1 with amino acid residues 1257-1411 representing the minimal region of EEA1 able of early endosomal targeting (Stenmark et al., 1996). Images of live cells were captured at 37ºC using an Axiovert 200M microscope with a heated stage equipped with a LSM 5 LIVE laser scanning microscope and a 100x/1.45 NA oil alpha Plan-Fluar objective. CFP-, -YFP and Cy5-flouresence were obtained using the 405 nm-, 488 nm- and 633 nm-diode lasers, respectively.

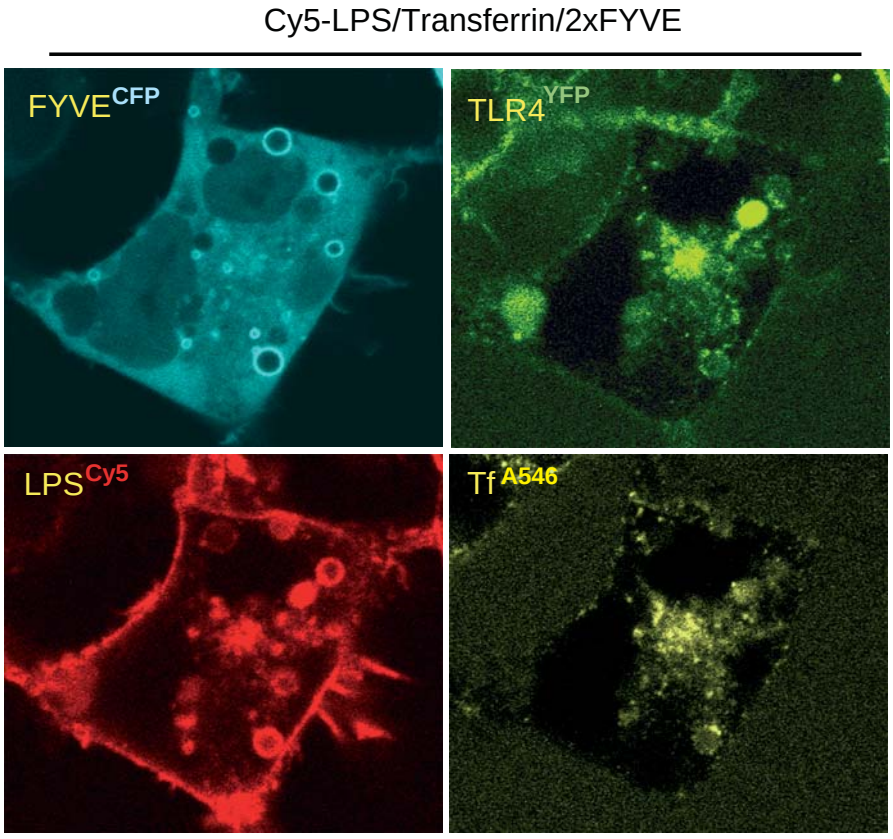

Supplementary Information, Figure 2.
LPS is internalized on early/sorting endosomes containing TLR4. HEK293 cells expressing $TLR4^{YFP}$ and MD-2 co-transfected with CD14 and a marker for early/sorting endosomes, $2xFYVE^{CFP}$. Confocal images of a cell 45 minutes after simultaneously addition of Alexa546-labeled transferrin Tf^{A546} (5µg/ml) and LPS^{Cy5} (250 ng/ml) addition. Confocal images presented are the full captures of the four separate channels presented in Figure 2e. Bar=5 µm.

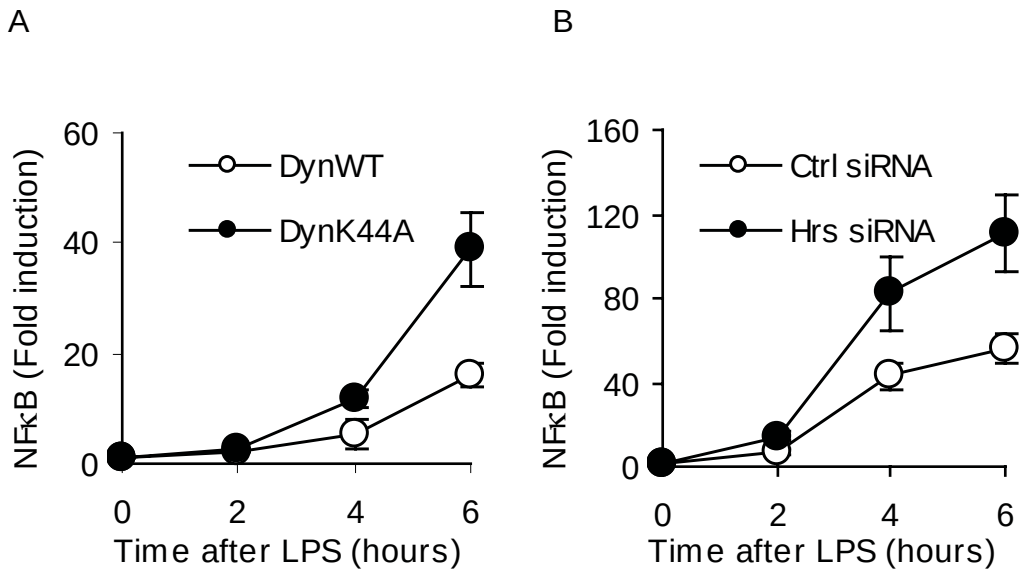

Supplementary Information, Figure 3.
Time kinetics of NFκB-activation with DynK44A and Hrs siRNA and controls.
HEK293 cells expressing TLR4^{YFP}/MD-2 were transfected with Elam-luc together with wild type dynamin (DynWT) or a dominant negative dynamin (DynK44A) (A), or treated with 40 nM Hrs siRNA or control siRNA for 48 hours before being transfected with Elam-luc together with CD14 (B). LPS-induced NFκB-activation was monitored after 0, 2, 4 and 6 hours of stimulation with LPS (10 ng/ml).

Methods: SiRNA duplexes targeting the coding region of Hrs and a non-interfering scrambled RNA duplex have previously been described (Bache et al., 2003). The siRNA duplexes used were synthesised by Dharmacon. HEK293 cells expressing TLR4^{YFP}/MD-2 were transfected with 40 nM siRNA for 48 hours using Oligofectamine (Invitrogen) according to the manufacturer's protocol. For the introduction of plasmid DNA into the siRNA transfected cells, the cells were replated and transfected for 24 hours using the GeneJuice transfection reagent.

Supplementary Information, Movie 1

Movie clip of a fusion event between two LPS positive endosomes. HEK293 cells stably expressing $TLR4^{YFP}$/MD-2 were transfected with CD14 and incubated with 300ng/ml LPS^{Cy5}. The movie was captured approximately 45 min after addition of LPS. The real time length of the movie is 245 s. Images of live cells were captured at 37 °C using an Axiovert 200M microscope with a heated stage equipped with a LSM 5 LIVE laser scanning microscope and a 100x/1.45 NA oil alpha Plan-Fluar objective. Cy5-flouresence was obtained using a 633 nm- diode laser.